## International Journal of Technology



http://ijtech.eng.ui.ac.id

Research Article

# Synthesis of a Polyvinylidene Fluoride Membrane with Polyethylene Glycol Additive for the Wastewater Treatment of Batik Industry

Sutrasno Kartohardjono<sup>1\*</sup>, Eva Fathul Karamah<sup>1</sup>, Arifina Febriasari<sup>2</sup>, Sherlyta Estella<sup>1</sup>, Michael Gabriel Owen<sup>1</sup>, Nickyta Tanryan<sup>1</sup>

**Abstract:** Polyvinylidene fluoride (PVDF) is a polymer widely used to prepare ultrafiltration membranes. However, PVDF membranes are hydrophobic; therefore, they have poor antifouling ability in filtration. Therefore, this study will modify PVDF membranes using N, N dimethyl acetamide (DMAc) solvents with polyethylene glycol (PEG) additives. The flat sheet membrane was prepared using the immersion precipitation method with PEG masses of 0, 0.5, 1, and 1.5 grams. The prepared membranes were then characterized using scanning electron microscopy (SEM), Fourier transform infrared spectroscopy (FTIR), contact angle, porosity, and tensile tests. Before being used as filtration feed, batik liquid waste was pretreated with PAC (poly aluminum chloride) coagulation-flocculation pretreatment. Furthermore, the batik liquid waste was filtered using PVDF/PEG membranes with feed pressures of 3, 4, and 5 bars. The permeate flux increased with the addition of PEG mass in the printing solution and operating pressure, ranging from 3.92 to 38.02 L/m2.h. However, this increase in flux decreased rejection because of the larger pore size, which allowed large particles to pass through the membrane. Rejection of TDS (Total Dissolved Solid), total suspended solid (TSS), turbidity, chemical oxygen demand (COD), and permeate color were in the range of 2.3%–9.3%, 0%-88.9%, 20.7%-65.5%, 44.5%-63.8%, and 18.3%-72.9%, respectively.

Keywords: Flux; PEG; PVDF; Rejection; Ultrafiltration

#### 1. Introduction

Propelled by the need for apparel and lifestyle products, the expansion of the batik sector in Indonesia generates liquid waste necessitating appropriate management (Munawir et al., 2024; Apriyanti et al., 2024). Batik wastewater is generally produced from the residual water resulting from the dyeing and washing processes. Chemicals, such as dyes, flour, oil, wax, lye, and detergents, are included in the effluent during the process (Rahmawati et al., 2016). These substances are typically non-biodegradable, resulting in their accumulation in soil and water, thus contaminating the ecosystem. Batik effluents are frequently vibrant and possess elevated levels of chemical oxygen demand (COD), biological oxygen demand (BOD), and both suspended and dissolved solids (Kusumawati et al., 2021).

<sup>&</sup>lt;sup>1</sup>Process Intensification Laboratory, Chemical Engineering Department, Faculty of Engineering, Universitas Indonesia, Kampus UI, Depok 16424, Indonesia

<sup>&</sup>lt;sup>2</sup>Chemical Engineering Department, Faculty of Engineering, Universitas Serang Raya, Serang, Indonesia \*Corresponding author's email: sutrasno@che.ui.ac.id, Telp.: +62217863516 ext. 204

Various techniques for the treatment of batik wastewater include biological treatment, adsorption, and ozonation; nevertheless, they are characterized by limited flexibility and high costs (Daud et al., 2022; Yeong Hwang et al., 2025). Membrane technology has emerged as a more eco-friendly and efficient option, particularly ultrafiltration membranes, which can eliminate color from batik wastewater (Jamil et al., 2024; Kartohardjono et al., 2024). Polyvinylidene fluoride (PVDF) is a polymer characterized by exceptional chemical and thermal resistance, making it appropriate for ultrafiltration membranes; however, its hydrophobic nature leads to fouling (Kartohardjono, Salsabila, et al., 2023; Subasi and Cicek, 2017). The incorporation of chemicals such as polyethylene glycol (PEG) can enhance the membrane's resistance to fouling and its hydrophilic characteristics (Ilyas et al., 2019). This study examined the impact of varying the PEG mass on PVDF membranes used for batik waste ultrafiltration. Membrane characterization testing included Fourier transform infrared spectroscopy (FTIR), scanning electron microscopy (SEM), contact angle measurement, porosity assessment, and tensile strength evaluation. The effectiveness of waste removal was assessed using COD, total dissoved solid (TDS), total suspended solid (TSS), pH, color, and turbidity, along with adjustments in feed pressure on the membrane. This study seeks to identify an effective solution for waste management in the batik industry using modified membrane technology, which is anticipated to promote sustainable growth and enhance the quality of life of the community.

### 2. Materials and Metchods

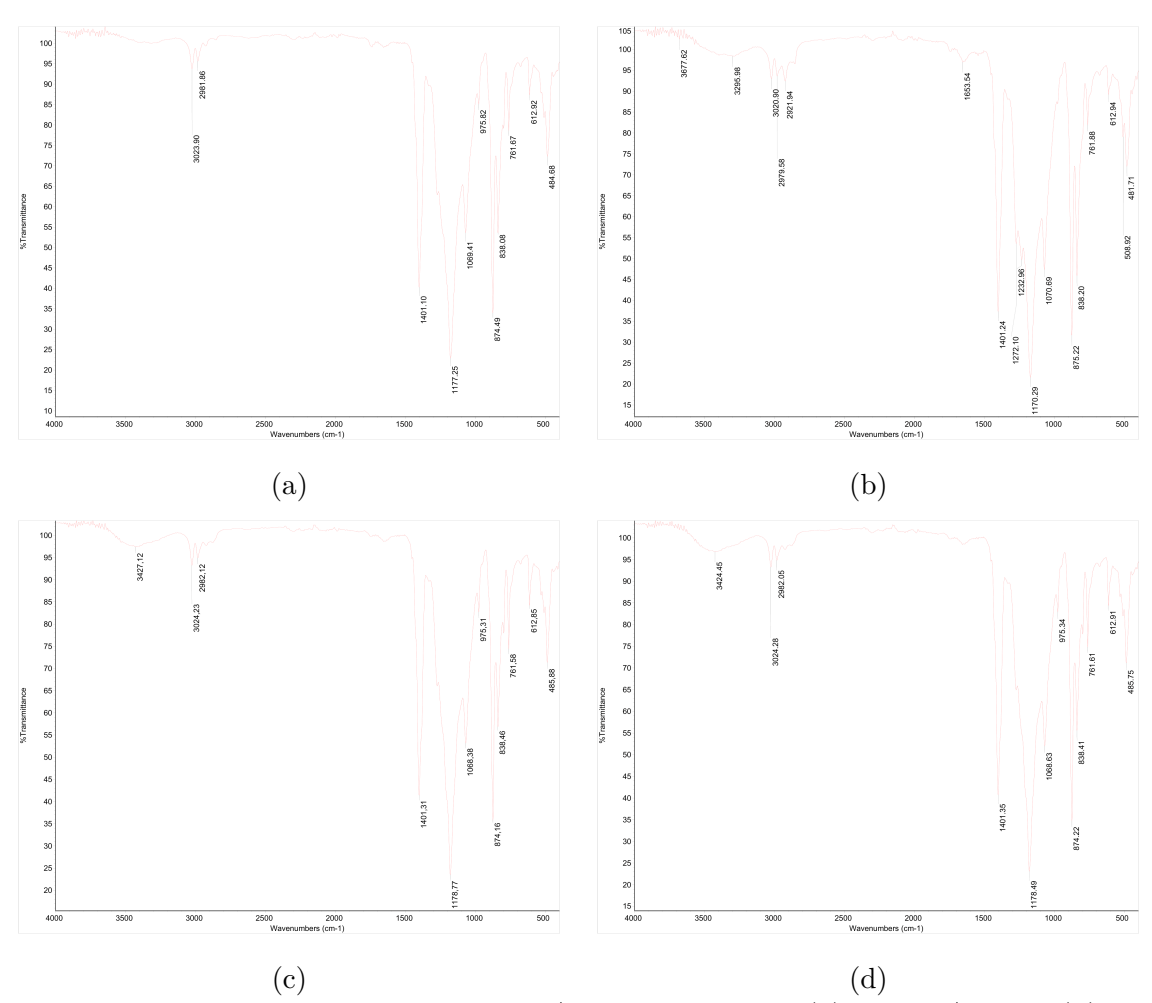
All chemicals employed for membrane fabrication were of analytical grade, with PVDF, PEG, and DMAC sourced from Solvay Chemical USA, Sigma-Aldrich Indonesia, and Merck Indonesia, respectively. Ethanol and deionized water were procured from Dwinika Intan Mandiri, Indonesia. The phase inversion technique is typically employed to fabricate flat sheet membranes (Ren et al., 2010). The membrane was synthesized by dissolving polyvinylidene fluoride (PVDF) in DMAc, incorporating PEG as an additive. The formulation consists of 15% PVDF + PEG and 85% DMAc, with PEG concentrations of 0, 0.5, 1.0, and 1.5. DMAc was initially placed in an Erlenmeyer flask, followed by the gradual addition of PVDF and PEG while stirring at 200 rpm and 25 °C. During the dissolution process, the polymer and additives were completely dissolved by gradually increasing the temperature to 60°C and the stirring speed to 300 rpm (Purnawan et al., 2021). The stirring was continued at 500 rpm for approximately 3 h until the solution achieved homogeneity. The homogeneous PVDF/PEG solution, designated as the casting solution, was subsequently allowed to rest at ambient temperature to facilitate bubble removal until the foam was eradicated. The casting solution was applied to the glass film using a casting-glass roller and then immersed in deionized water for approximately 24 h. The manufactured flat sheet membrane was subsequently immersed in 96 wt. % ethanol solution for 30 min and 50 wt. % ethanol solution for 1 h, and then dried in ambient air at room temperature for characterization.

Various techniques, including Fourier transform infrared spectroscopy (FTIR), scanning electron microscopy (SEM), and membrane mechanical strength examinations, are employed to assess alterations in the physical and chemical properties of membranes. The chemical composition of the membrane surface, mechanical strength, and surface morphology and cross-section of the membranes were analyzed using SEM, ZEISS Ultra 60, Thermo Scientific FTIR, Diamond Nicolet IS 5, and Universal Testing Machine, UTM 10 kN, respectively. Using a digital camera (Angle Meter) and the dry-wet mass method, the water contact angle and membrane porosity were measured simultaneously.

#### 3. Results and Discussion

#### 3.1 Membrane Characterization

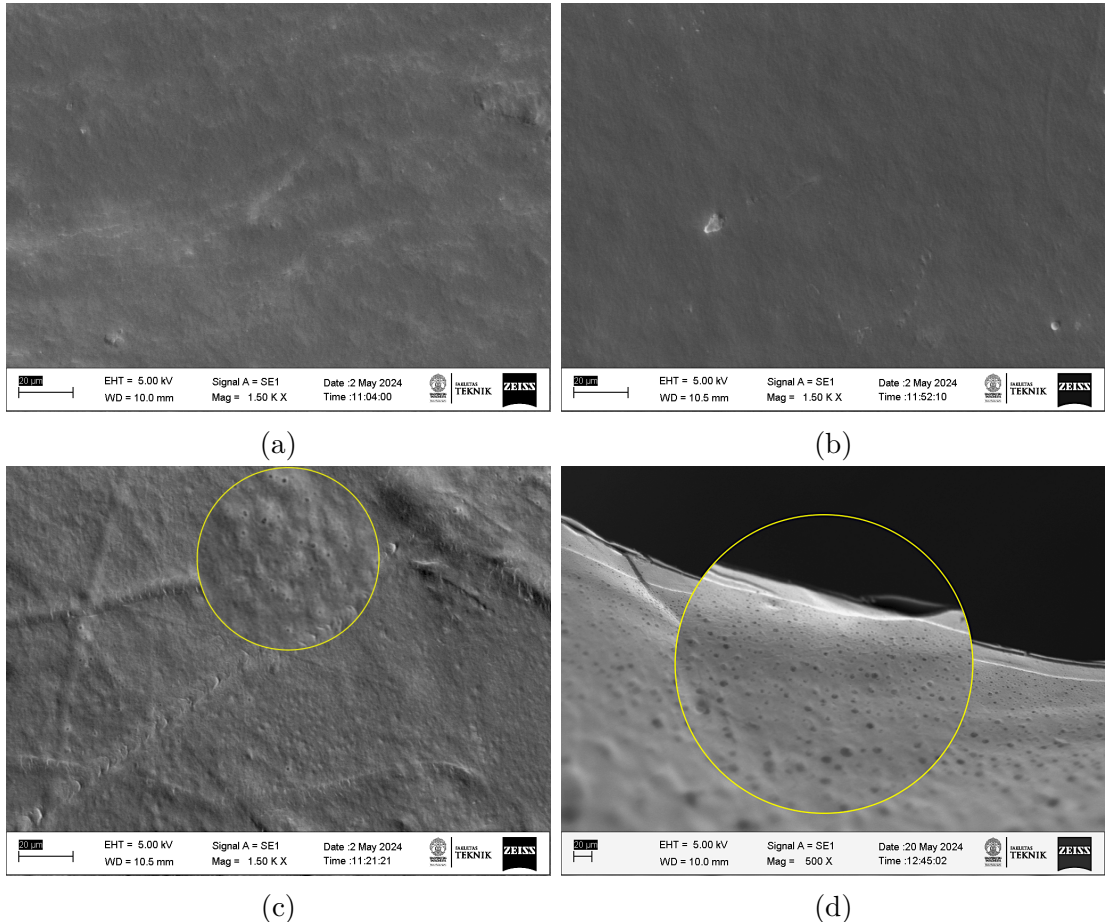
The chemical structure and functional groups of the produced membranes were identified using Fourier transform infrared spectroscopy (FTIR) spectra, as illustrated in Figure 1. The FTIR spectra of membranes, whether devoid of or containing PEG, are nearly identical because PVDF is the predominant component. The PVDF spectrum exhibits absorption at 761 and 1170 - 1178 cm-1, signifying the bending and stretching vibrations of CF2 (Abid et al., 2024). The peak at 1068 - 1070 cm-1 signifies the bending vibration of CF. The FTIR results of pure PVDF membranes exhibit differences with varying PEG additions, as evidenced by a broad absorption peak in the wavenumber range of 3295 - 3427 cm-1, indicative of hydroxyl group (O - H) vibrations, a characteristic functional group of PEG. The PVDF/PEG membrane can interact with water, functioning as a hydrophilic membrane (Nishiyama et al., 2016).



**Figure 1** FTIR spectrum of PVDF/PEG membranes (a) PVDF/PEG<sub>0</sub>; (b) PVDF/PEG<sub>0.5</sub>; (c) PVDF/PEG<sub>1.0</sub>; (d) PVDF/PEG<sub>1.5</sub>

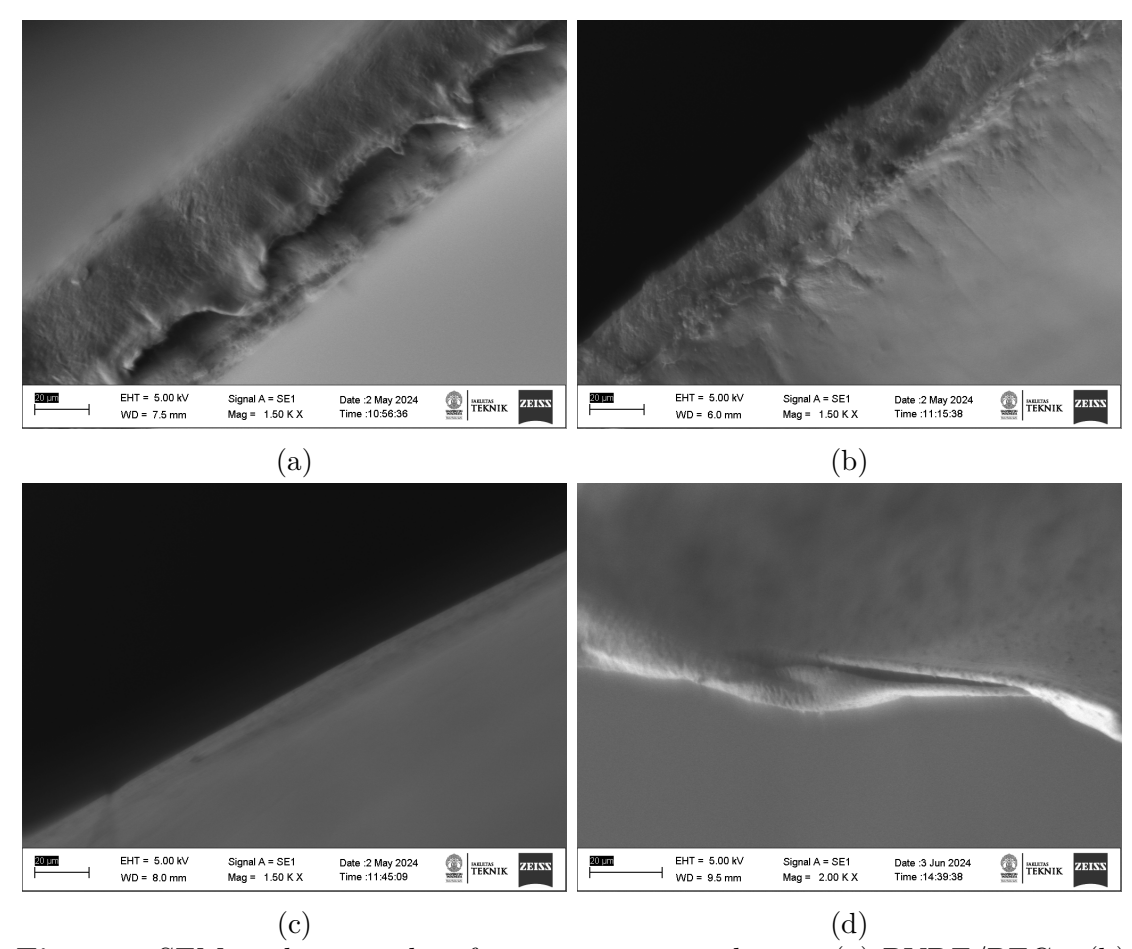
The SEM test results for the membranes PVDF/PEG<sub>0</sub>, PVDF/PEG<sub>0.5</sub>, PVDF/PEG<sub>1.0</sub>, and PVDF/PEG<sub>1.5</sub> are presented in Figure 2. The surface of the pure PVDF membrane is notably smooth and exhibits minimal porosity due to the absence of PEG addition. The PVDF/PEG<sub>0.5</sub> membrane exhibits a rougher surface; nevertheless, the difference is negligible compared to PVDF/PEG<sub>0</sub>. The pores on the surfaces of the PVDF/PEG<sub>0</sub> and PVDF/PEG<sub>0.5</sub> membranes are not distinctly observable; nevertheless, the incorporation

of PEG increases the surface roughness. Pore size augmentation can be inferred from the enhancement in membrane surface roughness (Woo et al., 2015). Meanwhile, irregularly distributed holes manifest on the  $PVDF/PEG_{1.0}$  membrane. The  $PVDF/PEG_{1.5}$  membrane possesses a very porous architecture and exhibits the highest roughness among all the samples. This demonstrates that PEG is crucial in pore creation within the membrane and enhances its hydrophilicity, rendering it more appropriate for filtration applications (Sadeghi et al., 2018).



**Figure 2** SEM images of PVDF/PEG membranes (a) PVDF/PEG<sub>0</sub>; (b) PVDF/PEG<sub>0.5</sub>; (c) PVDF/PEG<sub>1.0</sub>; (d) PVDF/PEG<sub>1.5</sub>

Figure 3 illustrates the membrane's cross-section, highlighting morphological alterations resulting from the incorporation of PEG mass. The incorporation of high-molecular-weight PEG into PVDF often results in a membrane architecture characterized by a dense, sponge-like bottom layer and a broad, porous top layer resembling fingers directed toward macrovoids (Casetta et al., 2023). A hydrophilic functional group known as PEG is included in the dope solution. It reduces the thermodynamic stability and accelerates the process of phase separation. It forms a membrane with a large number of holes. Furthermore, due to the hydrophilic nature of PEG, it facilitates the infiltration of non-solvents into the dope solution. Accelerates the solvent and non-solvent exchange rate during membrane formation in the coagulation bath. This rapid exchange accelerates the doped solution's precipitation rate, facilitates immediate demixing, and generates a porous membrane structure (Wongchitphimon et al., 2011). Figure 3 illustrates the SEM results for PVDF/PEG<sub>1.5</sub>, demonstrating that the incorporation of PEG resulted in the formation of large, irregular pores.



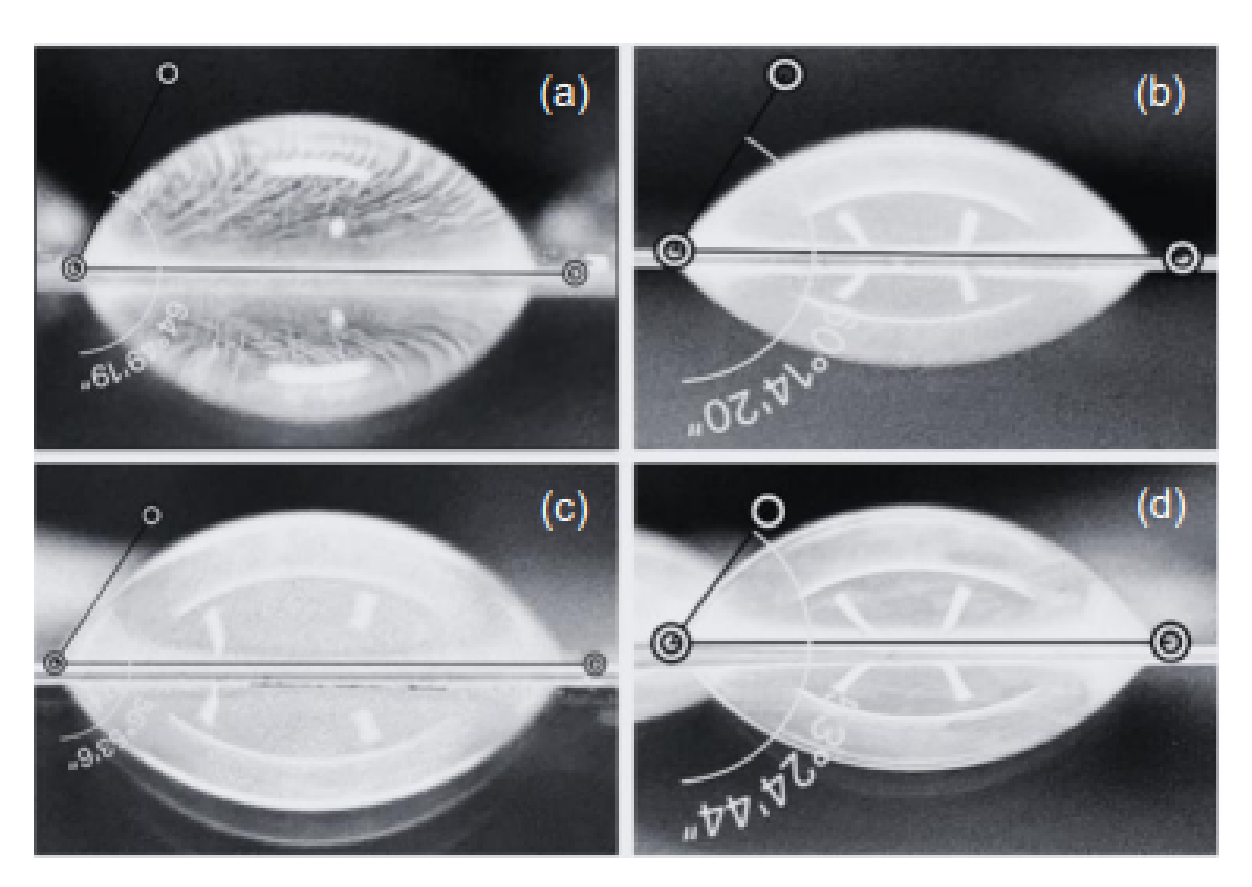
**Figure 3** SEM analysis results of cross section membranes (a) PVDF/PEG<sub>0</sub>; (b) PVDF/PEG<sub>0.5</sub>; (c) PVDF/PEG<sub>1.0</sub>; (d) PVDF/PEG<sub>1.5</sub>

Table 1 presents the membrane porosity assessment outcomes, indicating that a reduction in PVDF content or an increase in PEG content within the dope solution correlates with enhanced porosity. The hydrophobic nature and compact structure of PVDF diminish the membrane permeability as its concentration increases (Kang and Cao, 2014). The incorporation of PEG additives into the dope solution results in the PVDF/PEG membrane exhibiting a more pronounced thermodynamic impact than the kinetic effect, facilitating the formation of pores, as seen by the rise in porosity (Nguyen et al., 2023). The hydrophilic properties of PEG enhance the water infiltration into the dope solution and expedite the exchange between solvents and non-solvents. Simultaneously, the kinetic action induces an elevation in the viscosity of the solution with the incorporation of PEG, thereby decelerating the exchange rate and culminating in a more compact membrane structure (Su et al., 2023).

Table 1 Porosity of PVDF/PEG membranes

| Membrane type                      | Mean porosity (%) |  |
|------------------------------------|-------------------|--|
| $PVDF/PEG_0$                       | $28.2 \pm 3.0$    |  |
| $PVDF/PEG_{0.5}$                   | $30.5 \pm 5.8$    |  |
| $\mathrm{PVDF}/\mathrm{PEG}_{1.0}$ | $39.5 \pm 4.8$    |  |
| $PVDF/PEG_{1.5}$                   | $43.5 \pm 0.2$    |  |

Figure 4 The results of the membrane contact angle characterization are presented. All membranes exhibit hydrophilic properties, as indicated by their contact angles being less than 90° (Hebbar et al., 2017). PVDF/PEG<sub>0</sub> exhibits the highest hydrophobicity among the membranes analyzed, characterized by a contact angle of approximately 65.3°. This property is attributed to its surface composition, which includes C-F bonds that hinder hydrogen bond formation with water molecules (Guo et al., 2021). Meanwhile, the contact angles of the PVDF/PEG<sub>0.5</sub>, PVDF/PEG<sub>1.0</sub>, and PVDF/PEG<sub>1.5</sub> membranes were approximately 62.3°, 57.3°, and 53.3°, respectively, suggesting an increase in the hydrophilicity of the membranes. An increase in the PEG content within the membrane component corresponds to a decrease in the PVDF content, which enhances the surface hydrophilicity of the membrane due to the entrapment of PEG in the membrane matrix. This alteration modifies the hydrophobic characteristics of the PVDF membrane, rendering it more hydrophilic (Huev Ping et al., 2014).



**Figure 4** The contact angle of PVDF/PEG membranes (a) PVDF/PEG<sub>0</sub>; (b) PVDF/PEG<sub>0.5</sub>; (c) PVDF/PEG<sub>1.0</sub>; (d) PVDF/PEG<sub>1.5</sub>

The mechanical properties of the membrane indicate how well it can withstand the pressure applied during testing. Figs. 5 and 6 show the tensile strength and strain variation of the prepared membrane. Decreasing the PVDF concentration decreases the tensile strength of the membrane (Ali et al., 2018). The PVDF/PEG<sub>0</sub> membrane exhibited the highest tensile strength, at approximately 11.1 MPa. The elastic properties of the PVDF membrane can be seen from its high strain value. The higher the PVDF concentration, the tighter the distance between the polymer chains, making the membrane stiffer, more compact, and resistant to deformation. Therefore, the strain decreases because the PVDF/PEG<sub>0</sub> membrane has the lowest strain. In contrast, the PVDF/PEG<sub>1.5</sub> membrane has the highest strain. However, the tensile strength of the PVDF/PEG<sub>1.5</sub> variation is

higher than that of PVDF/PEG<sub>1.0</sub>, indicating that the distribution of pores in the membrane is not exhaustive and that its tensile strength tends to be stronger. The tensile strength of the PVDF membrane varies with the concentration and application. For water filtration applications, the expected tensile strength values range from 3.43 to 14.34 MPa (Sriyanti et al., 2023). Therefore, the resulting membrane meets these criteria.

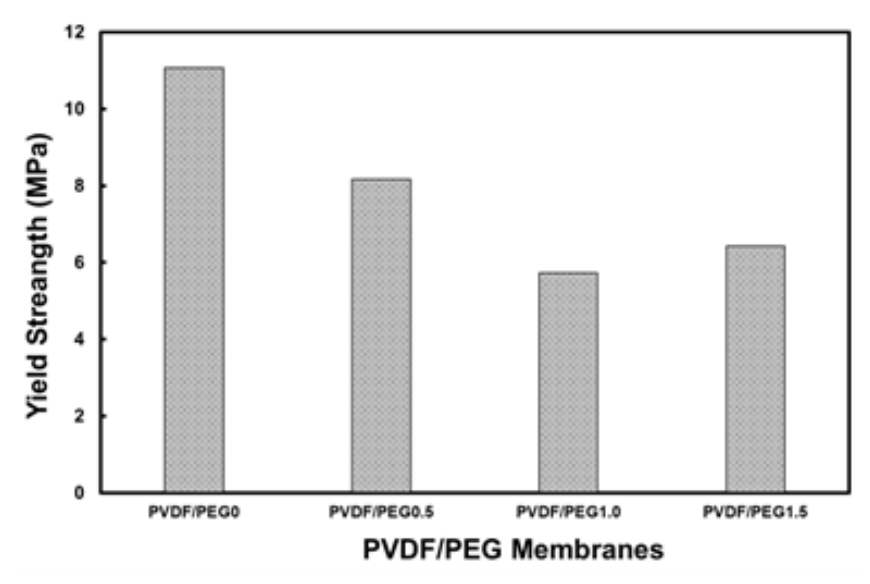


Figure 5 The yield strength of PVDF/PEG membranes

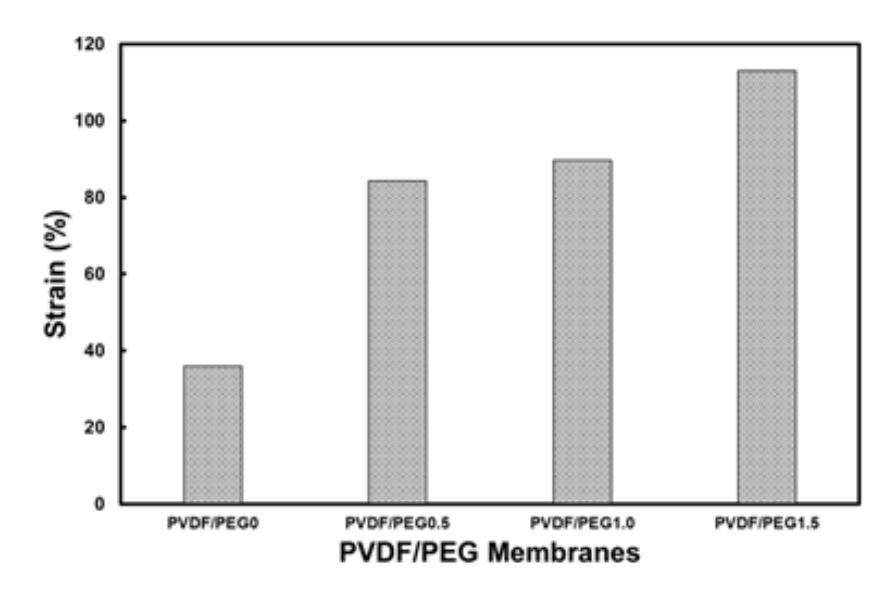


Figure 6 The strain of PVDF/PEG membranes

#### 3.2 Membrane Characterization

The batik effluent originated from the rolling and dyeing processes in a batik industry in Yogyakarta, Indonesia. The preliminary batik waste was characterized to provide a baseline for evaluating the efficacy of waste treatment using coagulation-flocculation and ultrafiltration using a membrane. The analyzed waste exhibited characteristics such as COD, TDS, TSS, color, turbidity, and pH. The batik wastewater was filtered through a cloth to eliminate large particles and subsequently diluted at a five-to-one ratio. Dilution

was implemented as an initial waste treatment to mitigate the impacts of waste contamination and decrease the waste concentration during the coagulation-flocculation process for maximum performance. Table 2 displays the attributes of the batik wastewater upon dilution.

Following dilution, the batik wastewater was subjected to a pretreatment procedure using coagulation-flocculation, facilitated by a jar test apparatus for agitation. The pretreatment process removes large particles before the waste is used for ultrafiltration feed. The coagulant used in this process is PAC, with a dose of 500 ppm and at pH 4.0 to run optimally (Kartohardjono, Karamah, et al., 2023). The initial batik waste is alkaline, so the pH must be reduced to 4.0 using an H2SO4 solution. The wastewater is stirred rapidly at 200 rpm for 4 min to form flocs because contact and collisions between particles cause clumping of dissolved solid particles. Subsequently, it is continued with slow stirring at 40 rpm for 10 min so that small flocs combine into larger flocs. After stirring, the waste is left for 30 min so that the macrofloc can fall to the bottom and be filtered. Watman 42 filter paper and Buchner funnel were used to speed up the filtering process. Subsequently, the pretreatment waste was clarified and adjusted to a pH of 7.0 using NaOH solution to ensure its safe disposal into the environment. This procedure results in the formation of silt, necessitating the subsequent filtration of the waste through filter paper. It can be used as a feed for ultrafiltration with a membrane. Table 2 shows the characterization of batik waste before and after the pre-treatment process. The pre-treatment technique significantly decreased pollutants in waste in all parameters, including COD (56.1%), TSS (95.5%), color (77.6%), and turbidity (84.7%). However, it had little impact on TDS since the pH 4.0 setting process promoted salt production by adding acid to the already alkaline waste. It also occurred at pH 7.0 at the end, raising the COD, TDS, color, and turbidity in the wastewater.

After dilution Parameter pH 4.0 After pH 7.0 coagulationflocculation рН  $10.9 \pm 0.2$  $4.02 \pm 0.2$  $4.1 \pm 0.2$  $7.01 \pm 0.2$ COD (mg/L)  $1005 \pm 12$  $954 \pm 11$  $174 \pm 2$  $442 \pm 5$ TSS (mg/L) $200 \pm 5$  $380 \pm 10$  $8.0 \pm 0.2$  $9.0 \pm 0.3$ TDS (mg/L)  $860 \pm 8$  $928 \pm 9$  $690 \pm 7$  $817 \pm 9$ Color (Pt-Co)  $2394 \pm 15$  $7155 \pm 45$  $508 \pm 5$  $536 \pm 6$ Turbidity  $190 \pm 6$  $490 \pm 15$  $23.0 \pm 1.0$  $29 \pm 1.3$ (FAU)

**Table 2** The characteristics of batik wastewater after dilution

The batik wastewater was treated via ultrafiltration (UF) using permeation cells with a membrane area of approximately 15.5 cm<sup>2</sup>. The water flow for UF operations was conducted for 20 min at different pressures, as shown in Figure 7. The incorporation of PEG into the PVDF membrane enhanced the membrane flux, with the PVDF/PEG<sub>1.5</sub> variant exhibiting the greatest flux value among the other configurations at identical pressure conditions. Conversely, the lowest flow value was recorded for the PVDF/PEG<sub>0</sub> membrane, as PVDF is a hydrophobic polymer, making water adsorption on the membrane surface challenging (Zou and Lee, 2022). The incorporation of PEG additives into the PVDF membrane introduces hydrophilic groups (–OH) that can engage in hydrogen bonding with water molecules, facilitating their passage across the membrane and thereby enhanc-

ing the membrane's flux value (Ismail et al., 2020). The PEG molecules that occupy the membrane matrix also solubilize in water, creating membrane gaps during the phase inversion process. The development of pores on the membrane surface facilitates water passage across the membrane, thereby enhancing the flux value. Figure 7 illustrates that the flow escalates with increasing pressure across all PEG concentrations. Enhanced pressure expedites water movement from the feed side to the permeate side, thereby augmenting the flux. Furthermore, heightened pressure results in more pronounced membrane holes, facilitating the passage of additional dissolved chemicals from the batik wastewater across the membrane. It diminishes the rejection capacity of the membrane, a critical characteristic in ultrafiltration.

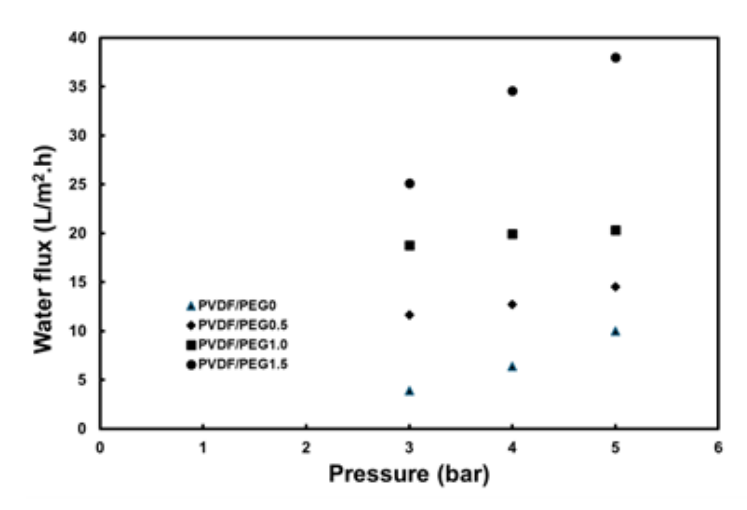


Figure 7 Water flux of PVDF/PEG membranes

Figure 8 illustrates the impact of variations in PVDF/PEG mass and pressure on the pH of the water flux resulting from the ultrafiltration process. The pH range of the ultrafiltration results of the batik wastewater was 7.13 - 7.41. The water flux pH tended to increase compared with the initial pH but was still close to the initial pH of the wastewater, which was 7.01. This shows that neither the variation in PVDF/PEG mass nor the operating pressure used in this study significantly affected the pH because the pores of the ultrafiltration membrane cannot hold ions that affect the pH. However, the permeate pH for each variation in PVDF/PEG mass and pressure has met the government's quality standards for textile waste pH, which is between 7 and 9 (Febriasari et al., 2021).

Figure 9 (see supplementary file) depicts the influence of PVDF/PEG mass and pressure fluctuations on the TSS rejection of batik wastewater from ultrafiltration. The PVDF/PEG<sub>0</sub> membrane achieved the highest TSS rejection, ranging from 55.6% to 88.9%. The range of TSS rejection percentages for the PVDF/PEG<sub>0.5</sub>, PVDF/PEG<sub>1.0</sub>, and PVDF/PEG<sub>1.5</sub> membranes were 33.3 to 66.7%, 11.1% to 44.4%, and 0% to 22.2%, respectively. The removed solids consisted of colloidal particles from the coagulation-flocculation process that were not successfully filtered by the filter paper. The PVDF/PEG<sub>0</sub> membrane at a pressure of 3 bar produced the highest TSS rejection, with a TSS reaching 1 mg/L because the membrane has the smallest pore size. As pressure increases, the permeate rate rises, and the pore size becomes more pronounced, allowing suspended particles in the waste that were previously trapped by the membrane to traverse it, resulting in an increase in total suspended solids (TSS) and a reduction in rejection efficiency (Malmali et al., 2018).

Figure 10 (see supplementary file) shows the effect of the PVDF/PEG mass and pressure variations on the turbidity rejection of batik wastewater in the UF process. Sim-

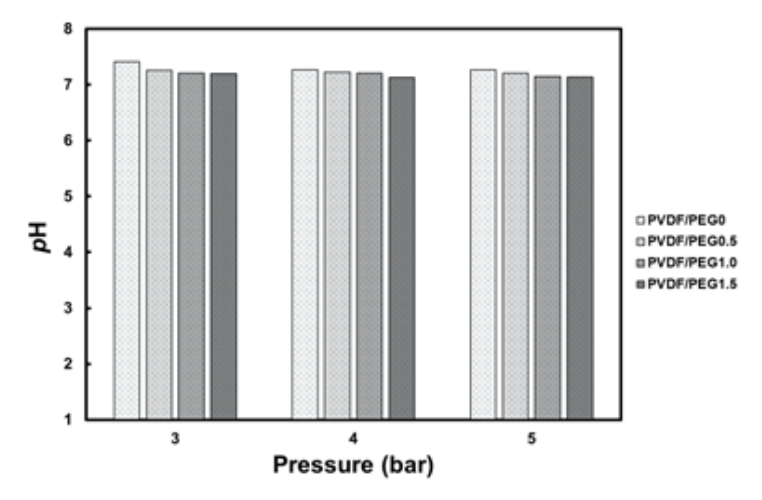


Figure 8 The effect of PVDF/PEG mass fraction and pressure on pH of water flux in the UF process

ilar to TSS, turbidity rejection decreases with increasing process pressure and PEG mass because TSS is directly proportional to turbidity. The decrease in TSS value indicates a reduction in turbidity in the permeate because the presence of solid particles gives a turbid effect on the waste (Hansen et al., 2021). The lowest turbidity removal was obtained using the PVDF/PEG<sub>1.5</sub> membrane at a pressure of 5 bar, which was only around 20.69%. Meanwhile, the ultrafiltration process produced the highest turbidity removal of 65.52% with a PVDF/PEG<sub>0</sub> membrane at a pressure of 3 bar. Higher rejection at low pressure is caused by particles in the feed running stably through the membrane without force in the form of additional pressure.

Figure 11 (see supplementary file) shows the effect of PVDF/PEG mass and pressure variations on TDS rejection in batik wastewater from the UF process. Overall, increasing the PVDF/PEG mass and pressure decreases the TDS rejection percentage. The highest percentage of TDS rejection was obtained by the PVDF/PEG<sub>0</sub> membrane, which was between 7.1% and 9.3%. The TDS rejection percentages for the PVDF/PEG<sub>0.5</sub>,  $PVDF/PEG_{1.0}$ , and  $PVDF/PEG_{1.5}$  membranes were 6.7%-8.7%, 4.9%-8.1%, and 2.3%-3.7%, respectively. The main components of TDS are ions and small molecules that the ultrafiltration membrane cannot filter due to the larger pore size (Urošević and Trivunac, 2020). Nanofiltration and RO membranes are considered more effective in reducing TDS (Mousavi and Kargari, 2022). Membranes with higher PEG mass tend to have lower TDS rejection at all pressure levels tested. This is due to the increase in porosity and membrane pore size as the PEG mass increases (Fadaei et al., 2014). PVDF/PEG<sub>0</sub> membranes always have the highest rejection, while PVDF/PEG<sub>1.5</sub> always have the lowest rejection at any pressure because pressure affects the membrane's permeate rate and pore size. The higher the pressure, the more water flow along with particles is forced through the membrane, so the results are not optimal and the rejection percentage is reduced. Thus, PVDF/PEG<sub>0</sub> membranes with pressures of around 3-5 bar will be more effective for batik wastewater treatment applications requiring high TDS rejection. However, if the TDS rejection is not too significant, membranes with higher PEG compositions can be used to increase the flux.

Figure 12 (see supplementary file) illustrates the impact of PVDF/PEG mass and pressure fluctuations on the COD rejection of batik wastewater during UF. Across all pressure variations, the PVDF/PEG<sub>0</sub> membrane demonstrated the maximum COD rejection. The COD rejection at a pressure of 3 bar was approximately 63%, which diminished

to 47% when the pressure was increased to 5 bar. However, pressure changes did not significantly affect rejection. The pore size and distribution influence the ultrafiltration rejection coefficient more than the operating parameters, such as pressure and feed flow rate (Polyakov and Zydney, 2013). At the same pressure, the percentage of COD rejection and the increase in PEG mass tend to decrease. The incorporation of PEG mass, a pore-forming agent, results in an increase in both pore size and membrane porosity; thus, a higher PEG concentration in the dope solution correlates with greater porosity values (Gayatri et al., 2023). Batik wastewater exhibits a high COD value due to the presence of synthetic dyes, salts, and organic compounds ranging from 1 to 2000 nm (Kanegsberg and Kanegsberg, 2011). The mean pore diameter of a pure PVDF membrane ranges from 60 to 150 nm (Basko et al., 2023). Consequently, diminutive color particles and organic compounds present in batik waste might permeate the membrane pores, resulting in suboptimal COD rejection.

Figure 13 (see supplementary file) shows the effect of PVDF/PEG mass and pressure on Pt-Co color rejection in the batik wastewater UF process. The higher the operating pressure and PEG mass in the dope solution component, the lower the color rejection of batik wastewater, where the highest color rejection is achieved by the PVDF/PEG<sub>0</sub> membrane at a pressure of 3 bar. The density of the membrane's pores is affected by the PEG mass; the denser and more regular the membrane's pores are, the better the membrane is for the color removal process (Abdulsalam et al., 2020). Meanwhile, increasing the operating pressure increases the flow velocity on the membrane surface, which increases the solute's mass transfer coefficient through the UF membrane pores. As a result, the solute concentration in the permeate increases, and as a result, membrane rejection decreases. The color rejection in batik wastewater is relatively low, between 16% and 27%, because the ultrafiltration membrane cannot filter color pigments well (Zakaria et al., 2023).

Figure 14 (see supplementary file) shows the batik wastewater after several stages of processing. The initial batik liquid wastewater is solid black. After dilution and pH adjustment of 4, the wastewater color becomes lighter because its concentration is reduced. The next stage is the coagulation-flocculation process, which changes the wastewater color to bright yellow and clear. At pH 7, the color of the wastewater remains the same, but white deposits appear due to the addition of NaOH to increase the pH. Finally, the wastewater from ultrafiltration with PVDF/PEG<sub>0</sub> membranes and a pressure of 3 bars produces water with a brighter yellow color and no white deposits. Therefore, the best removal percentage for all parameters was achieved at a pressure of 3 bar using PVDF/PEG<sub>0</sub> membranes. The permeate flow properties of the ultrafiltration process of batik liquid wastewater using PVDF/PEG<sub>0</sub> membranes at a pressure of 3 bars can be seen in Table 3. Although the flux is relatively low, the efficiency can be increased by installing several ultrafiltration membranes in parallel to produce a higher permeate volume (Shi et al., 2014). The pH and TDS parameters are not used as a reference in determining the optimal pressure and composition because the rejection percentage is relatively low, i.e., 10%, so it does not significantly affect the operating conditions of the ultrafiltration process. Based on Table 3, all parameters follow the quality standards of the government of the Republic of Indonesia, except for COD, which still requires further processing to reduce its levels.

| Parameter       | After dillution | After coagulation-flocculation | After UF       | Government<br>Regulation | Rejection (%)  |
|-----------------|-----------------|--------------------------------|----------------|--------------------------|----------------|
| рН              | $10.9 \pm 0.2$  | $4.1\pm0.2$                    | $7.3 \pm 0.1$  | 6 - 9                    | $4.4\pm1.1$    |
| COD (mg/L)      | $1005\pm12$     | $174\pm2$                      | $179\pm16$     | 150                      | $59.4 \pm 3.8$ |
| TSS (mg/L)      | $200 \pm 5$     | $8.0 \pm 0.2$                  | $2.67 \pm 1.5$ | 50                       | $70.4 \pm 2.3$ |
| TDS (mg/L)      | $860 \pm 8$     | $690 \pm 7$                    | $753 \pm 10$   | 2000                     | $7.9 \pm 1.2$  |
| Color (Pt-Co)   | $2394 \pm 15$   | $508 \pm 5$                    | $393\pm7$      | NA                       | $26.6 \pm 1.3$ |
| Turbidity (FAU) | $190 \pm 6$     | $23.0 \pm 1.0$                 | $11.3\pm1.5$   | 25                       | $60.9 \pm 5.3$ |

Table 3 The characteristics of batik wastewater after dilution

#### 4. Conclusion

The incorporation of Polyethylene Glycol (PEG) into the membrane dope solution substantially influences the structure and characteristics of the membrane. It increases the number of pores in the membrane, expands the pore dimensions, and enhances the hydrophilicity of the membrane while diminishing its tensile strength. The use of PEG in the doping solution enhances the mass transfer flow in the water permeate; however, it diminishes the rejection efficiency of total dissolved solids (TDS), total suspended solids (TSS), chemical oxygen demand (COD), turbidity, and color, while also causing a modest reduction in pH. In the ultrafiltration process, elevated feed pressure enhances water flux while diminishing the rejection of TSS, COD, turbidity, and color, and marginally raises the pH. Given the issues related to changes in polyethyleneglycol (PEG), further research should concentrate on effective membrane-cleaning technologies that can restore functionality while minimizing membrane degradation. Future studies focused on cleaning and maintaining PEG-modified membranes can enhance their operational viability and efficiency, thereby advancing membrane technology in water treatment processes.

#### Acknowledgements

The authors would like to express their gratitude to the Directorate General of Higher Education, Research, and Technology, Ministry of Education, Culture, Research, and Technology, for providing financial support for the study through Universitas Indonesia under Contract No. NKB-967/UN2.RST/HKP.05.00/2024.

#### Conflict of Interest

The authors declare no conflicts of interest.

### References

Abdulsalam, M., Che Man, H., Goh, P., Yunos, K., Abidin, Z., Isma, M., & Ismail, A. (2020). Permeability and antifouling augmentation of a hybrid pvdf-peg membrane using nano-magnesium oxide as a powerful mediator for pome decolorization. *Polymers*, 12. https://doi.org/10.3390/polym12030549

- Abid, M., Gzara, L., Wahab, R., Ahmed, I., Baig, N., Shamim, A., & Salam, M. (2024). Surface modification for enhanced anti-wetting properties of electrospun omniphobic membranes in membrane distillation. *Journal of Applied Polymer Science*, 141. https://doi.org/10.1002/app.55739
- Ali, I., Bamaga, O. A., Gzara, L., Bassyouni, M., Abdel-Aziz, M. H., Soliman, M. F., Drioli, E., & Albeirutty, M. (2018). Assessment of blend pvdf membranes, and the effect of polymer concentration and blend composition [PubMed ID: 29510555]. *Membranes*, 8(1), 13. https://doi.org/10.3390/membranes8010013
- Apriyanti, E., Susanto, H., & Widiasa, I. (2024). Preparation and performance evaluation of tio2 incorporated fly ash-kaolin ceramic membrane for oil/water separation. International Journal of Technology, 15, 1959. https://doi.org/10.14716/ijtech.v15i6.6294
- Basko, A., Lebedeva, T., Yurov, M., Ilyasova, A., Elyashevich, G., Lavrentyev, V., Kalmykov, D., Volkov, A., & Pochivalov, K. (2023). Mechanism of pvdf membrane formation by nips revisited: Effect of precipitation bath nature and polymer–solvent affinity. *Polymers*, 15, 4307. https://doi.org/10.3390/polym15214307
- Casetta, J., Virapin, E., Pochat-Bohatier, C., Bechelany, M., & Miele, P. (2023). Polymeric hollow fiber (hf) mixed matrix membranes (mmms): Mutual effect of graphene oxide (go) and polyvinylpyrrolidone (pvp) on nano-structuration. *Colloids and Surfaces A: Physicochemical and Engineering Aspects*, 681, 132805. https://doi.org/10.1016/j.colsurfa.2023.132805
- Daud, N. M., Abdullah, S. R. S., Hasan, H. A., & Dhokhikah, Y. (2022). Integrated physical-biological treatment system for batik industry wastewater: A review on process selection. *Science of The Total Environment*, 819, 152931. https://doi.org/10.1016/j.scitotenv.2022.152931
- Fadaei, A., Salimi, A., & Mirzataheri, M. (2014). Structural elucidation of morphology and performance of the pvdf/peg membrane. *Journal of Polymer Research*, 21. https://doi.org/10.1007/s10965-014-0545-x
- Febriasari, A., Huriya, Ananto, A., Suhartini, M., & Kartohardjono, S. (2021). Polysulfone–polyvinyl pyrrolidone blend polymer composite membranes for batik industrial wastewater treatment. *Membranes*, 11, 66. https://doi.org/10.3390/membranes11010066
- Gayatri, R., Syimir, A., Yuliwati, E., Cchem Mrsc, T. D. M., Jaafar, J., Zulkifli, M., Taweepreda, W., & Yahaya, A. (2023). Preparation and characterization of pvdf–tio2 mixed-matrix membrane with pvp and peg as pore-forming agents for bsa rejection. Nanomaterials, 13, 1023. https://doi.org/10.3390/nano13061023
- Guo, Y., Liu, C., Xu, W., Liu, G., Xiao, K., & Zhao, H.-Z. (2021). Interpenetrating network nanoarchitectonics of antifouling poly(vinylidene fluoride) membranes for oil—water separation. RSC Advances, 11(51), 31865–31876. https://doi.org/10.1039/D1RA05970J
- Hansen, D. S., Bram, M. V., Lauridsen, S. M. Ø., & Yang, Z. (2021). Online quality measurements of total suspended solids for offshore reinjection: A review study. *Energies*, 14(4), 967. https://doi.org/10.3390/en14040967
- Hebbar, R., Isloor, A., & Ismail, A. (2017). Contact angle measurements. In *Membrane characterization* (pp. 219–255). Elsevier. https://doi.org/10.1016/B978-0-444-63776-5.00012-7
- Huey Ping, N., Ahmad, A. L., Low, S. C., & Seng, O. (2014). The influence of peg additive on the morphology of pvdf ultrafiltration membranes and its antifouling properties

- towards proteins separation. Jurnal Teknologi, 70. https://doi.org/10.11113/jt. v70.3430
- Ilyas, H., Shawuti, S., Siddiq, M., Niazi, J. H., & Qureshi, A. (2019). Peg functionalized graphene oxide-silver nano-additive for enhanced hydrophilicity, permeability and fouling resistance properties of pvdf-co-hfp membranes. *Colloids and Surfaces A: Physicochemical and Engineering Aspects*, 579, 123646. https://doi.org/10.1016/j.colsurfa.2019.123646
- Ismail, N., Salleh, W., Ismail, A., Hasbullah, H., Yusof, N., Aziz, F., & Jaafar, J. (2020). Hydrophilic polymer-based membrane for oily wastewater treatment: A review. Separation and Purification Technology, 233, 116007. https://doi.org/https://doi.org/10.1016/j.seppur.2019.116007
- Jamil, P. A. S. M., Aziz, N. A., Bashir, M. J., Aziz, H. A., & Hung, Y.-T. (2024). Treatment of textile effluent. In *Industrial waste engineering* (pp. 43–86). Springer. https://doi.org/10.1007/978-3-031-46747-9\_12
- Kanegsberg, B., & Kanegsberg, E. (2011). Handbook for critical cleaning: Applications, processes, and controls. CRC Press. https://doi.org/10.1201/b10621
- Kang, G.-d., & Cao, Y.-m. (2014). Application and modification of poly(vinylidene fluoride) (pvdf) membranes a review. *Journal of Membrane Science*, 463, 145–165. https://doi.org/10.1016/j.memsci.2014.03.055
- Kartohardjono, S., Karamah, E., Siahaan, G., Ghazali, T., & Lau, W. (2023). The simultaneously removal of nox and so2 processes through a polysulfone hollow fiber membrane module. *International Journal of Technology*, 14, 576. https://doi.org/10.14716/ijtech.v14i3.5544
- Kartohardjono, S., Karamah, E. F., Hayati, A. P., Talenta, G. N., Ghazali, T. A., & Lau, W. J. (2024). Effect of oxidants in the utilization of polysulfone hollow fiber membrane module as bubble reactor for simultaneously removal of nox and so2. *International Journal of Technology*, 15(1), 63–74. https://doi.org/10.14716/ijtech.v15i1.6415
- Kartohardjono, S., Salsabila, G., Azzahra, R., Purnawan, I., & Lau, W. (2023). Preparation of pvdf-pvp composite membranes for oily wastewater treatment. *Membranes*, 13, 611. https://doi.org/10.3390/membranes13060611
- Kusumawati, N., Rahmadyanti, E., & Sianita, M. (2021). Chapter 3 batik became two sides of blade for the sustainable development in indonesia. In S. K. Sharma (Ed.), Green chemistry and water remediation: Research and applications (pp. 59–97). Elsevier. https://doi.org/https://doi.org/10.1016/B978-0-12-817742-6.00003-7
- Malmali, M., Askegaard, J., Sardari, K., Eswaranandam, S., Sengupta, A., & Wickramasinghe, S. R. (2018). Evaluation of ultrafiltration membranes for treating poultry processing wastewater. *Journal of Water Process Engineering*, 22, 218–226. https://doi.org/https://doi.org/10.1016/j.jwpe.2018.02.010
- Mousavi, S., & Kargari, A. (2022). Water recovery from reverse osmosis concentrate by commercial nanofiltration membranes: A comparative study. *Desalination*, 528, 115619. https://doi.org/10.1016/j.desal.2022.115619
- Munawir, H., Kausar, M., Pratiwi, I., & Kholid Alghofari, A. (2024). Managing and mitigation of risk at batik laweyan during the covid-19 pandemic. *International Journal of Technology*, 15, 561. https://doi.org/10.14716/ijtech.v15i3.5276
- Nguyen, T. D. T., Altiok, E., Siekierka, A., Pietrelli, A., & Yalcinkaya, F. (2023). Preparation and characterization of microfiltration membrane by utilization non-solvent induced phase separation technique. *Journal of Membrane Science and Research*, 9(2), 1995689. https://doi.org/10.22079/JMSR.2023.1995689.1594

- Nishiyama, T., Sumihara, T., Sato, E., & Horibe, H. (2016). Effect of solvents on the crystal formation of poly(vinylidene fluoride) film prepared by a spin-coating process. *Polymer Journal*, 49. https://doi.org/10.1038/pj.2016.116
- Polyakov, Y. S., & Zydney, A. L. (2013). Ultrafiltration membrane performance: Effects of pore blockage/constriction. *Journal of Membrane Science*, 434, 106–120. https://doi.org/https://doi.org/10.1016/j.memsci.2013.01.052
- Purnawan, I., Angputra, D., Debora, S., Karamah, E., Febriasari, A., & Kartohardjono, S. (2021). Polyvinylidene fluoride membrane with a polyvinylpyrrolidone additive for tofu industrial wastewater treatment in combination with the coagulation–flocculation process. *Membranes*, 11, 948. https://doi.org/10.3390/membranes11120948
- Rahmawati, F., Permadani, I., & Pasha, D. (2016). The composite of zro2-tio2 produced from local zircon sand used as a photocatalyst for the degradation of methylene blue in a single batik dye wastewater. *Bulletin of Chemical Reaction Engineering Catalysis*, 11, 133–139. https://doi.org/10.9767/bcrec.11.2.539.133-139
- Ren, J., Zhou, J., & Deng, M. (2010). Morphology transition of asymmetric flat sheet and thickness-gradient membranes by wet phase-inversion process. *Desalination*, 253(1), 1–8. https://doi.org/https://doi.org/10.1016/j.desal.2009.12.001
- Sadeghi, I., Kaner, P., & Asatekin, A. (2018). Controlling and expanding the selectivity of filtration membranes. *Chemistry of Materials*, 30. https://doi.org/10.1021/acs.chemmater.8b03334
- Shi, X., Tal, G., Hankins, N. P., & Gitis, V. (2014). Fouling and cleaning of ultrafiltration membranes: A review. *Journal of Water Process Engineering*, 1, 121–138. https://doi.org/https://doi.org/10.1016/j.jwpe.2014.04.003
- Sriyanti, I., Fandu Ramadhani, R., Almafie, M., Idjan, M., Syafri, E., Solihah, I., Sanjaya, M., Jauhari, J., & Fudholi, A. (2023). Physicochemical and mechanical properties of polyvinylidene fluoride nanofiber membranes. Case Studies in Chemical and Environmental Engineering, 9, 100588. https://doi.org/10.1016/j.cscee.2023.100588
- Su, W.-C., Ho, J., Gettel, D., Rowland, A., Keating, C., & Parikh, A. (2023). Kinetic control of shape deformations and membrane phase separation inside giant vesicles. Nature Chemistry, 16, 1–9. https://doi.org/10.1038/s41557-023-01267-1
- Subasi, Y., & Cicek, B. (2017). Recent advances in hydrophilic modification of pvdf ultrafiltration membranes a review: Part i. *Membrane Technology*, 2017(10), 7–12. https://doi.org/https://doi.org/10.1016/S0958-2118(17)30191-X
- Urošević, T., & Trivunac, K. (2020, January). Achievements in low-pressure membrane processes microfiltration (mf) and ultrafiltration (uf) for wastewater and water treatment. In *Current trends and future developments on (bio-) membranes* (pp. 67–107). Elsevier. https://doi.org/10.1016/B978-0-12-817378-7.00003-3
- Wongchitphimon, S., Wang, R., Jiraratananon, R., Shi, L., & Loh, C. H. (2011). Effect of polyethylene glycol (peg) as an additive on the fabrication of polyvinylidene fluoride-co-hexafluropropylene (pvdf-hfp) asymmetric microporous hollow fiber membranes. *Journal of Membrane Science*, 369(1), 329–338. https://doi.org/https://doi.org/10.1016/j.memsci.2010.12.008
- Woo, S. H., Park, J., & Min, B. (2015). Relationship between permeate flux and surface roughness of membranes with similar water contact angle values. Separation and Purification Technology, 146. https://doi.org/10.1016/j.seppur.2015.03.048
- Yeong Hwang, T., Chai, M., Ling Shing, W., Ong, M., & Rajamani, R. (2025). Optimizing microwave-assisted extraction of carbohydrate from scenedesmus sp. cultivated in

- domestic was tewater. International Journal of Technology, 16, 255. https://doi.org/10.14716/ijtech.v16i1.7301
- Zakaria, N., Rohani, R., wan mohtar, H., Purwadi, R., Sumampouw, G., & Indarto, A. (2023). Batik effluent treatment and decolorization—a review. *Water*, 15, 1339. https://doi.org/10.3390/w15071339
- Zou, D., & Lee, Y. M. (2022). Design strategy of poly(vinylidene fluoride) membranes for water treatment. *Progress in Polymer Science*, 128. https://doi.org/10.1016/j.progpolymsci.2022.101535